Realizing the potential of polyethylene oxide as new positive tribo-material: Over 40W/m2 high power flat surface triboelectric nanogenerators

Realizing the potential of polyethylene oxide as new positive tribo-material: over 40 W/m^2 high power flat surface triboelectric nanogenerators

Peng Ding[a,†], Jinkai Chen[a,†], Umar Farooq[a], Pengfei Zhao[b], Navneet Soin[b], Liyang Yu[c*], Hao Jin[a], Xiaozhi Wang[a], Shurong Dong[a] and Jikui Luo[c,b*]

[a]Coll. of Info. Sci. & Electron. Eng., Zhejiang University, 38 Zheda Road, Hangzhou 310027, China.
[b]Inst. of Renew. Energy & Environ. Technol., Bolton University, Deane Road, Bolton BL3 5AB, UK
[c]Key Lab of RF Circuits and Systems, Hangzhou Dianzi University, Hangzhou 310018, China

[†] These authors contributed equally to the work.
*Corresponding authors emails: yuliyang@hdu.edu.cn, jl2@bolton.ac.uk

Abstract:

The on-going research into the negative tribo-materials has led to significant improvements in the performance of triboelectric nanogenerators (TENGs), however, very little attention has been paid for positive tribo-materials. This work reports on the use of poly(ethylene oxide) (PEO) as the positive tribo-material for the fabrication of TENGs and shows that PEO has much higher positive tribo-polarity than the existing choice of polyamide-6 (PA6). A 2 × 2 cm^2 TENG comprising of spin-coated flat PEO and polydimethylsiloxane (PDMS) films produces a voltage of up to 970 V, a current density of 85 mAm^{-2}, and a power of ~40 Wm^{-2} under a 50 N contact force. Comparatively, the PA6/PDMS TENG only produces 630 V, 30 mAm^{-2}, and a power of ~18 Wm^{-2}, showing the remarkable property of the PEO as the positive tribo-material. The results are further supported by the contact potential difference between PEO (1.26 V) and PA6 (0.87 V) obtained using Kelvin Probe Force microscopy. Furthermore the triboelectric behavior of PEO is explained in the context of the positively charged oxygen functional groups and the lower work function of PEO as compared to PA6. The work thus expands the current portfolio of materials used for triboelectric nanogenerators with great prospects.

Keywords: triboelectric nanogenerator, poly(ethylene oxide), polyimide (PA6 Nylon), high surface potential, high triboelectric affinity.

1. Introduction

With the development of intelligent electronic devices, such as smart portable/wearable devices, wireless sensor networks and so on, renewable and sustainable power sources, that can be utilized to build battery-free systems, are becoming increasingly important. Since the power consumption of these electronic systems is of hundreds of microwatts to tens of milliWatt levels, it is possible to power these electronic systems by harvesting ubiquitous ambient small-scale waste mechanical energy. Microgenerators based on piezoelectric [1-3], electromagnetic [4], pyroelectric [5] effects have been intensively studied and exploited for such applications. Triboelectric nanogenerators (TENGs), invented by Wang *et al* in 2012 [6], can convert the available mechanical energy such as vibration [7], wind [8, 9] and waves [10, 11] into usable electric energy, have gained great attention since then owing to their very high power output, excellent energy conversion efficiency and cost-effectiveness.

The TENGs have three basic operating modes: two electrode contact [12], single electrode contact [13] and sliding modes [14], with the first one being the preferred one owing to its simple architecture and high performance. The contact mode TENGs typically consist of two insulators with electric polarities far apart in the triboelectric series [15], *i.e.* upon contact and subsequent separation, one material has a high ability to donate electrons (hereafter called as the positive tribo-material), while the other material has a high ability to gain electrons (called as the negative tribo-material). Current efforts for the development of TENG technology mainly focus on the enhancement of the output power *via* an increase in the surface charge density. To this effect, the recent approaches rely on: (i) judicious selection of triboelectric materials, (ii) modification of tribo-materials, for instance, surface patterning with micro-/nano-structures [16], chemical surface functionalization [17], and nanoparticles-filled or pore-formed polymers [18-20], (iii) charge injection [21] or use of polarized piezoelectric nanomaterials [22], and (iv) use of hybrid structures, such as piezoelectric/triboelectric structures [23], solar cell/triboelectric structure [24], and electromagnetic/triboelectric structures [25]. Of all the above mentioned methods, except for the judicious use of materials, the rest of the methods rely on time-consuming, complicated processes or structures, and/or use expensive equipment, and thereby lead to an increase in

the cost of the TENGs. For instance, the nano/micro-structured surfaces and injected charges tend to deteriorate with operation due to damage of the microstructures and thus may not provide the required stability and reliability of the devices, whereas the hybrid structures have the potential for high conversion efficiency [26], but are yet to achieve satisfactory results. Consequently, the selection of the optimal materials with high electron affinity difference is the simplest and most effective way to improve the performance of TENGs, but is currently restricted by the limited choices of existing materials.

Vigorous investigations have shown that polydimethylsiloxane (PDMS), polyvinylidene fluoride (PVDF) and polytetrafluoroethylene (PTFE) are among the best negative tribo-materials for high performance TENGs owing to their strong negative electron affinity [27-29]. On the contrary, not much attention has been paid to the selection of positive tribo-materials, even though they are equally important as the negative tribo-materials for enhancing the surface charge density and subsequent power density. It is clear from the triboelectric series, there are only very limited choices for positive insulator tribo-materials and mostly metals such as aluminum (Al) and copper (Cu) have been used as positive tribo-materials [30-32]. However, these metals do not rank high in triboelectric series in their ability to donate electrons. For example, flat surfaced Cu/PTFE TENG shown in the literature was shown to have a charge density of 40 μCm^{-2} only [33], much smaller than those of other reported TENGs. Several other positive triboelectric insulator materials have been employed to construct TENGs, such as silk [34], carbon nanotubes (CNTs) [35], glass [36] and polyamide-6 (PA6, Nylon) with varying degrees of success [37]. The silk/PET TENG obtained a maximum peak power density of only 10 mWm^{-2}, while the CNTs/PDMS TENG produced about 5 Wm^{-2} which was mainly attributed to the high surface area of CNT arrays [35]. Among the positive triboelectric insulator materials, PA6 is regarded as the best choice for making high performance TENGs as it has a strong positive tribo-polarity in triboelectric series. Our earlier works utilizing PA6 as the positive tribo-material against poly(vinylidene fluoride), PVDF, was shown to perform excellently, providing an open-circuit voltage, V_{OC}, of 520 V, and a short-circuit current density, J_{SC}, of 2.7 mAm^{-2} [37]. Similarly, in this work, using PA6 against a PDMS counter-surface, the PA6/PDMS TENG was shown to provide a V_{OC} of 630 V and J_{SC} of 30 mAm^{-2} (corresponding a surface charge density of 110 μCm^{-2}),

with an effective maximum peak power density of 18 Wm^{-2}. It is apparent that the search for positive materials for TENGs is lagging far behind that of negative tribo-materials and thus warrants the question: is there any other low-cost material which possesses higher positive polarity for enhancing the power output and surface charge density of TENGs?

Polyethylene oxide (PEO) is a synthetic, low-cost commodity polymer which is also bio-compatible and water-soluble [38]. Here, we report for the first time on the use of pristine PEO films as the positive tribo-material to fabricate high performance TENGs in combination with PDMS. Relying on a simple spin-coating process without the added complication of micro/nano-fabrication process, we demonstrate PEO/PDMS TENGs with a peak-to-peak V_{OC} of 970 V, a J_{SC} of 85 mAm^{-2} (corresponding a charge density of 154 μCm^{-2}), and a peak power density of ~40 Wm^{-2}, significantly higher than those of CNTs/PDMS and PA6/PDMS TENGs, and is one of the best performances reported yet for TENGs comprising of pristine flat membrane structures. The higher positive electronic affinity of the PEO films as compared to that of PA6 is further verified by Kelvin probe force microscopy (KPFM), as the contact potential difference (CPD) values for PEO and PA6 are 1.26 V and 0.87 V, respectively. And the voltage and current density of the PEO/PDMS TENG increase with the increase in contact force, movement frequency and spacer distance. Considering the desirable properties of water solubility and bio-compatibility, we believe that the PEO based TENG devices have broad application prospects in implantable and bio-compatible electronic devices besides their use as high performance energy harvesters for conventional portable electronics.

2. Fabrication and experimental setup

2.1. Fabrication of triboelectric nanogenerators

The physical structure and the photo image of the contact-mode TENG are shown in Fig. 1(a), with the fabrication processes for PEO and PDMS films described in Figs. 1(b) and (c), respectively. Two pieces of acrylic (2 cm × 2 cm × 0.1 cm) plates were used as the substrates onto which a conductive, adhesive nickel (Ni) tape was glued on one side to act as the conductive electrode. To obtain PDMS films, a PDMS (184 Silicone Elastomer, Dow

Corning Co. Ltd.) solution was prepared by mixing the elastomer and cross-linker in a 10:1 ratio (w/w). The obtained solution was degassed prior to being spun onto the Ni electrode, initially at 500 rpm (rotations per minute) for 10 sec, followed by 1200 rpm for 10 sec. The as-obtained PDMS film was then thermally cured on a cleanroom paper on a hot plate at 105 °C for 40 min (note the temperature of the acrylic plate is lower than 105°C, and no deformation of the acrylic plate was observed). The thickness of the resulting PDMS films was measured to be ~140 μm, as confirmed using the profilometer.

PEO powders with different molecular weights (M_w) were purchased from Shanghai EKEAR Biological Technology Co. Ltd (China). The samples prepared using PEO of molecular weight (M_w) of 100000, 600000, 3000000 $g.mol^{-1}$, are hereafter designated as PEO10, PEO60, PEO300, respectively. The PEO powders were dissolved in deionized (DI) water at different mass concentrations of 12% for PEO10, 9% for PEO60 and 2% (w/w) for PEO300 owing to the fact that polymers with different molecular weights have different viscosity levels [38]. The resulting PEO solutions were spun on glass substrates at different rotation speeds between 500 – 1500 rpm for 10 sec to obtain the films with different thicknesses and subsequently dried in an oven at 55 °C for 3 hr. Finally, the dried PEO films were peeled off from the glass substrate and attached to adhesive Ni electrodes, as shown in Fig. 1(c).

For comparison, PA6/PDMS TENGs were also fabricated. The PA6 (pellets obtained from Rhodia Ltd.) membranes were prepared by a phase-inversion process, in accordance with earlier reports by Soin *et al* [37]. The obtained PA6 membranes with a thickness of ~150 μm were glued to the Ni conductive tapes to assemble the TENGs.

2.2. Experimental setup and Characterization

A dynamic fatigue tester system (Popwil Model YPS-1) was utilized to characterize the TENGs by controlling the contact force, frequency and spacer distance of two substrates of different materials. An oscilloscope (Tektronix MDO3022) with an internal load resistance of 100 MΩ was used to test the open-circuit voltage. The short circuit current was measured using a picoammeter (Keysight B2981A), with the corresponding current density obtained by dividing the active area of the TENGs. For all the measurements, the electrode of PEO side of

TENGs was connected to the positive side of the oscilloscope and picoammeter, with that of PDMS side of TENGs grounded. The measurements were conducted when the output performance of TENGs reached stable. In our experiments, the dynamic fatigue tester system contacts the two plates closely under a fixed force before dynamic contact and separation, which guarantees a full contact between them. This process reduces the time to reach the stable output, which is typically less than 100 cycles. In a typical test, the plate consisting of the positive tribo-material was moved vertically to make contact with the plate with negative tribo-material. The active area of TENGs characterized is 2 × 2 cm^2, unless specified. The Kelvin Probe Force Microscopy (KPFM) measurements were performed using the KPFM mode in an atomic force microscopy (AFM) system (Veeco Dimension 3100) with a Pt-coated Si probe. The measurements were carried out at oscillation amplitude of 3 V, resonance frequency of 150 kHz at a distance of 20 nm between the probe tip and sample. The Fourier Transform infrared spectroscopy (FTIR) spectra of PEO and PA6 samples were obtained using a Bruker TENSOR II at a nominal resolution of ±2 cm^{-1} for a total of 64 scans and the data was analyzed using the vendor-provided software, OPUS.

3. Results and Discussion

3.1. Performance of TENGs with different materials

Using PEO films of various thicknesses and molecular weights, we have evaluated the output performance of the PEO/PDMS TENGs to gain an understanding of the role of physico-chemical properties of PEO on its triboelectric properties. Furthermore, to assess its performance against the benchmark PA6 material, a comparison of PA6/PDMS and PEO/PDMS TENGs was carried out at a fixed working condition of 50 N impact force, 5 Hz working frequency and 4 mm spacer distance, with the results presented in Fig 2. Considering the effect of molecular weight first, Figs. 2(a) and (b) exhibit the peak-to-peak V_{OC} and charge density of the TENGs with PEO films with different molecular weights but approximately similar thickness of ~110 μm. The V_{OC} of the TENG with PEO300 film is 890 V, slightly less than those of the TENGs with PEO10 (930 V) and PEO60 (970 V) films respectively. The PEO molecular weight has a limited impact on the measured charge density

with values of 158 μCm^{-2}, 153 μCm^{-2} and 157 μCm^{-2}, for the TENGs prepared with PEO10, PEO60, PEO300 films, respectively. As the PEO60 films showed a slight higher output voltage, for further characterization we are only considering the PEO60 films unless specified. Upon varying the thickness of the PEO films, it can be seen that both the V_{OC} and J_{SC} have a similar variation trend with thickness as shown in Figs. 2(c) and (d). As the thickness of the PEO60 film increases from 60 to 110 μm, the peak-to-peak V_{OC} and J_{SC} concurrently increase from 800 to 970 V and 48 to 86 mAm^{-2}, respectively. However, it can be observed that the peak-to-peak V_{OC} and J_{SC} start to decay when the PEO film thickness increases continuously with the corresponding values of 865 V and 61 mAm^{-2} at a PEO film thickness of 150 μm, respectively. Thus, there exists an optimal thickness of the PEO film to maximize the electrical output of the TENGs. It can be explained that the thicker the friction layer, the more triboelectric charge that will be obtained [39]. When the thickness of friction layers reaches a certain value, the exceeding thickness does not contribute to the charge accumulation but rather enlarges the distance between triboelectrification charge and conducting layers, affecting the generation of electrostatic induction charge [39, 40]. It should be noted that the V_{OC} and charge density values obtained from the PEO/PDMS TENGs are significantly higher than those obtained from PA6/PDMS TENGs which only produced 630 V and a charge density of 110 μCm^{-2}. Based on these results, we can conclude that when measured against PDMS, the PEO films have a higher positive electron affinity as compared to PA6, and that the molecular weight has limited effect on electron affinity of PEO.

To further confirm the superior properties of PEO as the positive tribo-material for TENGs, a more specific and direct comparison between PEO60 and PA6 has been made. Fig. 3(a) shows the V_{OC} performance of a TENG prepared using the PEO/PA6 material combination, with the Ni electrode of the PEO side connected to the positive lead of the oscilloscope, while the PA6 side was grounded. The structure shows a positive voltage of ~30 V, indicating that PEO is more positive in triboelectric series than that of PA6. Fig. 3(b) shows the comparison of the V_{OC} and J_{SC} between the TENGs prepared with PDMS membranes in combination with PEO60 and PA6 films respectively. For both the cases, PDMS films were used as the negative tribo-material, and tested at the same condition of 50 N force, 5 Hz frequency and 4 mm spacer distance. It can be observed that both the peak-to-peak V_{OC} (970 V) and J_{SC} (85

mAm^{-2}) of the PEO60/PDMS TENG are significantly greater than those of the PA6/PDMS TENG (630 V, 30 mAm^{-2}). The significantly higher output of the PEO/PDMS TENG can thus be attributed to the higher positive electron polarity of the PEO material, and is further confirmed using the KPFM measurements as discussed later. The output powers of the PEO60/PDMS and PA6/PDMS TENGs were measured under different load resistances (R) with the instantaneous peak power calculated as $P=I^2R$. While the peak current of the PEO60/PDMS TENG is much higher than that of the PA6/PDMS TENG, as shown in Fig. 3(c), with the increase in the load resistance, the value of the peak current drops off quite rapidly. In fact, the instantaneous peak power density (Fig. 3(d)) reaches a value of 40 Wm^{-2} and 18 Wm^{-2} for the PEO60 and PA6 TENGs, respectively, both at a load resistance of about 200 MΩ. It is worth emphasizing that this reported value of ~40 Wm^{-2} is one of the best reported values for TENGs assembled using flat surface polymeric films. In fact, the value is approximately three orders of magnitude (10 mWm^{-2}) higher than that of the silk/PET TENG [34], about ten times higher than that (5 Wm^{-2}) of the CNTs/PDMS TENG [35], and even higher than that (35.6 Wm^{-2}) of the Al/PDMS TENG with nanostructured surface [16], demonstrating the superior performance of the PEO/PDMS TENGs. It should be mentioned that the PA6 membranes prepared using the phase inversion process contains a high density of pores as compared to those of dense films formed by casting and spin-coating processes, which produces significantly higher power outputs when is utilized in TENGs [37].

Based on the above results, in order to systematically assess the performance of PEO/PDMS TENGs, the electrical output of the PEO/PDMS (110 μm thick PEO60 film) TENG was studied, including the V_{OC} and J_{SC}, under varying impact forces, impact frequencies and spacer distances. Figs. 4(a) and (b) show the V_{OC} and J_{SC} of the PEO60/PDMS TENG at various contact forces of 30-90 N at a fixed driving frequency of 5 Hz and 4 mm spacer distance. It can be clearly observed that the V_{OC} increases steadily from 850 V (at 30 N) to 1070 V (at 70 N), and then slowly goes up to 1120 V (at 90 N force). The corresponding current density shows a similar trend with the increase of force, and rises from 70 mAm^{-2} to 100 mAm^{-2} as the contact force increases from 30 to 90 N. This observed increase in the electrical output as a function of contact force has been observed previously as well [36] and is attributed to the elastic nature of the contacting materials with an increase in the contact

force, which enhances the effective contact areas, thereby producing higher surface charge density and output power. The short circuit transferred charge density is one of the most important parameters for comparing the output of TENGs, and is calculated by integrating one cycle of short-circuit current pulse over time. At 50 N contact force, the charge density of the PEO60/PDMS TENG is 154 μCm^{-2} which further increases to 170 μCm^{-2} at a force of 90 N. From all the aforementioned values, it can be seen that as the contact force reaches a certain value (~80-90 N in this case), the increase in the contact area tends to saturate and the rise of voltage, current and transferred charge slowdown consequentially.

Figs. 4(c) and (d) show the V_{OC} and J_{SC} characteristics of the PEO60/PDMS TENG as a function of contact frequency at a working condition of 50 N contact force and 4 mm spacer distance. It can be clearly observed that both V_{OC} and J_{SC} show a similar trend wherein the values increases rapidly with working frequency from 1-5 Hz and saturates at higher impact frequency. In fact, the peak-to-peak V_{OC} increases from 530 to 1020 V when the frequency increases from 1 to 5 Hz, while the corresponding current density increases from 35 to 88 mAm^{-2}. Such trend of electrical output can be attributed to increased contact speed under higher frequency, leading to a faster transferring of electrons, hence higher current density and power outputs [37].

The effect of spacer distance on the V_{OC} and J_{SC} output of the PEO60/PDMS TENG was also studied at a fixed 50 N contact force and 5 Hz contact frequency as shown in Figs. 4(e) and (f). As the spacer distance is increased from 3 mm to 6 mm, the peak-to-peak V_{OC} rises from 920 V to 1090 V, and the corresponding current density increases from 67 mAm^{-2} to 92 mAm^{-2}. According to the previous work by Niu et al. [41], the V_{OC} of the contact-mode TENG increases with the increment of the spacer distance (x) and the inner surface charge density (σ) *via* the relationship$V_{OC} = (\sigma . x)/\varepsilon_o$. Moreover, at a fixed frequency, the larger spacer distance means a higher relative contact velocity of the PEO60 and PDMS films, which leads to a faster flow of electrons through the external circuit, thereby producing higher current density [36].

Furthermore, apart from PDMS, various other tribo-negative insulator materials such as fluorinated ethylene propylene (FEP), polyethylene terephthalate (PET), gelatin, and polycaprolactone (PCL) were used to confirm that the superior performance of the PEO as a

positive tribo-material is a general material property rather than specific to the PDMS. To maintain parity with the testing conditions, the TENG contact area was kept at 2 × 2 cm^2, and tested under the same conditions as those for the PEO/PDMS TENGs: 50 N force, 5 Hz and 4 mm spacer distance. Fig. 5(a) shows the comparison of the peak-to-peak V_{OC} for various assembled TENGs utilizing PEO60 and PA6 as the positive tribo-materials in combination with different negative tribo-materials (PET, FEP, PCL, Gelatin), respectively. It can be seen that for all of these negative tribo-materials, TENGs with PEO60 always shows higher performance than those with PA6 membrane. Accordingly, the charge density shows the same trend wherein the PEO60 film based TENGs show higher charge density, as shown in Fig. 5(b), thus proving the suitability of PEO against not only PDMS but also other negative tribo-materials.

As triboelectrification is a surface charging effect, the surface charge density of TENGs is expected to improve *via* surface treatment and nanostructuring. In order to demonstrate how surface modification and structuring can potentially improve the output performance of PEO60/PDMS TENGs, a facile method was adopted. The method involved spin coating of PEO60 and PDMS films on sand papers (P1200, MATADOR Co.) using the same conditions as that for the synthesis of flat surface films, then peeling them off from the sand papers and gluing to the conductive adhesive Ni electrodes, with the patterned side as the contact surfaces. Surface SEM images of the PDMS and PEO films with flat and rough surfaces are shown in Fig. S1 (Supporting Information). We produced this surface structured PEO60/PDMS TENGs and tested at 4 mm spacer and 5 Hz frequency at two contact forces (50 N, 90 N). For peak-to-peak V_{OC}, as compared to the TENGs comprising of flat surface films (970 V at 50 N and 1130 V at 90 N), the rough-surfaced TENGs showed a slight decrease in outputs (900 V at 50 N and 1070 V at 90 N), as shown in Fig. 5(c). However, for the rough-surfaced TENGs, the measured charge density showed significantly higher values of 217 μCm^{-2} at 50 N and 263 μCm^{-2} at 90 N, respectively, as compared to the flat-surfaced TENGs which displayed values of 154 μCm^{-2} under 50 N and 170 μCm^{-2} under 90 N, as shown in Fig. 5(d). It can be clearly observed that the surface roughness of the TENG has an evident effect on the charge density of TENGs, which is attributed to significant improvement of effective contact area for rough surface TENGs. However, the PEO/PDMS TENG with flat

surface has a slightly higher peak-to-peak V_{OC} than that of TENG with rough surfaces even it has much lower charge density. The reason is probably as follows. Since PDMS is soft with high viscosity, when the flat surface PDMS film contacts the flat surface PEO film, and they adhere very well. A relatively stronger force is needed to separate them, resulting in a faster instantaneous velocity of separation as compared to the rough surface case. This means a faster charge transferring speed through external circuit. According to the definition of current (I=dQ/dt) and voltage (V=IR, the voltage meter in our experiment is similar to a load resistance), the faster charge transferring speed can lead to a greater current and voltage value. Although the peak voltage decreases slightly for the rough-surfaced TENG, it should be noted that the total transferred charge increases significantly, so the roughness of the TENG surface leads to an improvement in the electrical performance of the PEO-based TENGs.

To assess the stability of the PEO based TENGs for self-powered systems, we operated the PEO60/PDMS TENG for over 20,000 cycles at a 5 Hz frequency for which the V_{OC} output is shown in Fig. 6. Within the 20,000 cyclic tests, no large deterioration of V_{OC} was observed, indicating that the PEO60/PDMS TENGs have excellent stability and reliability.

3.2. Mechanism for high performance TENGs with PEO film

For a contact-separation mode TENG, when the surfaces of two triboelectric materials (*i.e.* PEO and PDMS) are in contact under the influence of an external mechanical force, opposite triboelectric charges *i.e.* negative charges on the PDMS and positive charges on the PEO surfaces are generated on the two surfaces with the same density. Once the pressing force is released, the opposite charges on the two surfaces get separated from each other, leading to the establishment of the potential difference between the two electric plates. This potential difference will drive the electrons to flow between the two electrodes through an external circuit until the potential difference is fully offset by the transferred charges. A higher triboelectric surface charge density will produce not only a higher amount of charges transferred through the external load, but also a larger open-circuit voltage in each cycle. Thus, it is understandable that the output power and transferred charge density of a TENG strongly depends on the potential difference between the two material surfaces [42]. Also, it

is amply clear from the results shown above that as compared to PA6, the PEO shows a significantly higher positive tribo-effect. Let us now discuss the possible reasons for this behavior. To understand why the positive tribo-polarity of PEO polymer is greater than PA6, we characterized the surface potential between the PA6 and PEO with different molecular weights using KPFM [43].

According to the working principle of KPFM, the surface potential of a sample can be visualized as a voltage (V_{CPD}) applied between the tip and sample to nullify the contact potential difference (CPD), as schematically shown in Fig. 7**(**a). The work function of the sample, φ_{sample}, is defined as:

$$\varphi_{sample} = \varphi_{tip} - eV_{CPD} \quad (1)$$

where φ_{tip} is the work function of the tip, V_{CPD} is the measured contact potential difference (CPD) between the tip and the sample, and e is the electronic charge. Firstly, the energy levels of the tip and sample surface are presented in Fig. 7(b) <i>, with the aligned vacuum and different Fermi energy levels. Upon bringing the tip closer to the sample surface, the tip and sample surface come into electrical contact, causing the Fermi levels of the tip and sample to be aligned and thus reaching a steady-state equilibrium (as shown in Fig. 7(b) <ii>). An external V_{DC} is applied to the tip to nullify the electrical force, which has the same magnitude with the developed CPD, as shown in Fig. 7(b) <iii>. The amount of applied external bias V_{DC} that nullifies the electrical force due to the V_{CPD} is equal to the work function difference between the tip and sample. Therefore, it can be seen from Equation 1 that a higher V_{CPD} value represents a lower sample work function and it is known that for two materials with work functions of φ_1 and φ_2, if $\varphi 1 > \varphi 2$, then the $\varphi 1$ material will charge negative against the $\varphi 2$ material [44], while the material with $\varphi 2$ has a higher tendency to donate electrons. Previous work has reported for PEO, the work function has a value of ~3.95 eV, while that of PA6 is ~4.30 eV [44], and consequently the PA6 will charge negatively against the PEO. Indeed in the earlier section, we noted that a TENG comprising of PEO/PA6 combination, the structure showed a value of ~30 V, again indicating that the PEO is more positive. Fig. 7(c) shows the summary of the CPD values for the measured samples of PEO10, PEO60, PEO300 and PA6 in this work. For the PA6 film, the measured CPD value is 0.875 V, much lower than those obtained by the PEO films which displayed values of 1.190, 1.266 and

1.160 V for PEO10, PEO60 and PEO300, respectively. It can be seen that the molecular weight has only a limited effect on the surface potential, yet the PEO60 film shows a slightly higher CPD value than other two PEO films. As compared with PA6, a higher V_{CPD} value for the PEO means that PEO is more triboelectric positive, thus having a higher ability to donate electrons, and explains why the PEO/PDMS TENGs have higher outputs than that of PA6/PDMS TENGs. The detailed CPD images obtained by KPFM for the PA6, PEO10, PEO60, PEO300 films can be found in Fig. S2.

Since the surface potential of an organic material is mainly determined by its functional groups on its surface [45], FTIR measurements were conducted to investigate the functional groups on the PA6 and PEO films (see Fig. 8**(**a)). The peaks at 1340 and 1466 cm^{-1} originate from the vibrations of the CH_2 group. The strong band from 920 to 1200 cm^{-1} from PEO is attributed to the C-O-C bonds, that around 2880 cm^{-1} corresponds to the symmetric and asymmetric CH stretching, while that at 3560 cm^{-1} is from the OH group. It can be obviously seen that there is no significant difference between the PEO films with different molecular weights in the FTIR spectra, confirming that they have similar functional groups. This can explain the similar surface potential and triboelectric polarity for PEO10, PEO60, PEO300, and similar performance of TENGs with those PEO films. As for the PA6, the peaks are observed at 1545 and 3300 cm^{-1}, corresponding to the NH group, as shown in Fig. 8(b). The peak at around 1640 cm^{-1} is from the ketone group, and is the most prominent, while that around 2920 cm^{-1} belongs to the CH group but shows a smaller intensity than that for the PEO films. By looking at any of the published triboelectric series of materials in the literature, it can be observed that the nitrogen containing polymers, *i.e.* polymers with pyridine, amine and amide groups, develop the highest positive charge, whereas the halogenated polymers develop the most negative charge. For the PEO films, the surface oxygen functional groups can also provide a positive charge and has been reported in earlier report from Diaz et al [46]. And it is believed that the C-O-C stretching bonds is one possibility to form the a-CO:H bonds in a random fashion when H is bonded to an O [47]. Furthermore, PEO has the OH bonds on its original molecular structure. Therefore, PEO film offers highly dense C-O-C and OH bonds, which are expected to exhibit strongly tendency to repel electron from the surface because the H atoms have low electron affinity, resulting in more positive polarity in

triboelectric series for the PEO material [47].

3.3. Applications of the PEO/PDMS TENGs

The instantaneous power being delivered by the PEO/PDMS TENGs has been exploited for applications to power electronic devices. A 2 × 2 cm^2 PEO60/PDMS TENG was found to be able to directly light up hundreds of LEDs without any charge storage circuit as shown in Fig. 9**(**a) and in Supplementary video 1. For many applications, the pulsed AC nature of output current from TENGs at a large voltage is not very useful owing to the requirements of a constant DC current with low voltage amplitude for most cases. To overcome this, a standard charge circuit is typically used to store the charges produced by a TENG (Fig. 9(b) <i>) in a capacitor or a battery *via* a full-wave rectifier which is then used to power external electronic devices. However, this also poses a problem as the TENGs normally have very high optimal impedance (~200 MΩ in our study) with a voltage output of several hundreds of volts and low current density, leading to low efficiency in direct charging storage. In this work, we have adopted a fly-buck circuit to improve the storage rate of the TENG output as shown in Fig. 9(b) <ii>. The fly-buck converter itself is composed of a DB107S rectifier bridge, a BSS127 MOSFET transistor; a COTS coupled inductor with a 20:1 turn ratio, a MBRM110L Schottky diode, and a storage capacitor. The transistor is controlled by a signal nanogenerator. Figs. 9(c) and (d) show the charging curves for 22, 47 and 100 μF capacitors, respectively, by a standard circuit and the fly-buck circuit under 5 Hz, 50 N and 4 mm operation condition for the TENG. It is clear that the charging speed of the fly-buck circuit is much faster than the standard circuit. As the TENGs were operated at the same conditions, the fast charging means high conversion/storage efficiency. For example, while the voltage on the 100 μF capacitor rises from 0 V to 2 V in 5 sec using the fly-buck charging circuit, the standard circuit can only charge up to 0.04 V, corresponding to a charging speed of 0.4 Vs^{-1} and 0.008 Vs^{-1}, respectively, *i.e.* the charging speed of the fly-buck convertor is 50 times of the standard circuit! Due to the fast charging abilities of the fly-buck circuit, the TENGs can be used to drive electronic devices in real time. We utilized a 2×2 cm^2 PEO60/PDMS TENG working at a low frequency of 2 Hz, to drive electronic devices such as a commercial calculator and a

digital watch as shown in Figs. 9(e) and (f). After operating the TENG for only a few cycles, the calculator and the digital watch, whose internal coin cell batteries were removed, started to work. Even after the TENG stopped working, they can still work for times up to tens of minutes because of the energy stored in the capacitor (Supplementary video 2 and 3).

4. Conclusions

In summary, poly(ethylene oxide), for the first time has been explored for the fabrication of high-performance TENGs which as compared to the existing material of choice, polyamide-6, shows a higher positive electronic polarity. In fact, when used in conjunction with PDMS as the negative tribo-material, the flat-surfaced PEO/PDMS TENG produced a power output (40 Wm^{-2}, at 50 N contact force) more than twice that of the PA6/PDMS TENG (18 Wm^{-2}). Further exploration of the material properties and structure reveals that the electrical output is affected more by the thickness of the PEO film (optimal value of 110 μm) than by its molecular weight, while increasing the surface roughness led to a significant increase in the output charge density from 170 to 263 μCm^{-2} at 90 N of force. The improvement of the performance of the PEO/PDMS TENGs is mainly attributed to the high surface potential of PEO as confirmed by higher values of contact potential difference (CPD) measured using KPFM. The work unambiguously shows a simple, cost-effective way to improve the performance of TENGs by using PEO as the positive tribo-material. Taking into account the bio-compatibility and environmental-friendly nature of the PEO polymer, the PEO-based TENGs are not just good for powering electronics, but can also have broad future prospects for implantable and biodegradable electronic devices applications.

Acknowledgements

This work was supported by the following programs: National Natural Science Foundation of China (Nos. U1613202, U1609210，61376118 and 61674172), Zhejiang science and technology plan No.2016C31061 and Fundamental Research Funds for Central Universities(2016QNA5005, 2016XZZX001-005), National Key R&D program of China (2016YFC0801301).

References

[1] Z.L. Wang, J.H. Song, Science, 312 (2006) 242-246.

[2] P.K. Panda, J. Mater. Sci., 44 (2009) 5049-5062.

[3] R.M. Yu, C.F. Pan, J. Chen, G. Zhu, Z.L. Wang, Adv. Funct. Mater., 23 (2013) 5868-5874.

[4] I. Sari, T. Balkan, H. Kulah, Sens. Actuator A-Phys., 145 (2008) 405-413.

[5] S.R. Hunter, N.V. Lavrik, S. Mostafa, S. Rajic, P.G. Datskos, Review of pyroelectric thermal energy harvesting and new MEMs based resonant energy conversion techniques, in: N.K. Dhar, P.S. Wijewarnasuriya, A. Dutta (Eds.) Energy Harvesting and Storage: Materials, Devices, and Applications Iii, Spie-Int Soc Optical Engineering, Bellingham, 2012.

[6] F.R. Fan, Z.Q. Tian, Z.L. Wang, Nano Energy, 1 (2012) 328-334.

[7] W. Tang, T. Jiang, F.R. Fan, A.F. Yu, C. Zhang, X. Cao, Z.L. Wang, Adv. Funct. Mater., 25 (2015) 3718-3725.

[8] J. Bae, J. Lee, S. Kim, J. Ha, B.S. Lee, Y. Park, C. Choong, J.B. Kim, Z.L. Wang, H.Y. Kim, J.J. Park, U.I. Chung, Nature communications, 5 (2014) 9.

[9] Y. Yang, G. Zhu, H.L. Zhang, J. Chen, X.D. Zhong, Z.H. Lin, Y.J. Su, P. Bai, X.N. Wen, Z.L. Wang, ACS Nano, 7 (2013) 9461-9468.

[10] Z.H. Lin, G. Cheng, W.Z. Wu, K.C. Pradel, Z.L. Wang, ACS Nano, 8 (2014) 6440-6448.

[11] G. Zhu, Y.J. Su, P. Bai, J. Chen, Q.S. Jing, W.Q. Yang, Z.L. Wang, ACS Nano, 8 (2014) 6031-6037.

[12] G. Zhu, Z.H. Lin, Q.S. Jing, P. Bai, C.F. Pan, Y. Yang, Y.S. Zhou, Z.L. Wang, Nano Lett., 13 (2013) 847-853.

[13] J.K. Chen, P. Ding, R.Z. Pan, W.P. Xuan, D.P. Guo, Z. Ye, W.L. Yin, H. Jin, X.Z. Wang, S.R. Dong, J.K. Luo, Nano Energy, 34 (2017) 442-448.

[14] G. Zhu, J. Chen, Y. Liu, P. Bai, Y.S. Zhou, Q.S. Jing, C.F. Pan, Z.L. Wang, Nano Lett., 13 (2013) 2282-2289.

[15] G. Zhu, C. Pan, W. Guo, C.-Y. Chen, Y. Zhou, R. Yu, Z.L. Wang, Nano Lett., 12 (2012) 4960-4965.

[16] S.H. Wang, L. Lin, Z.L. Wang, Nano Lett., 12 (2012) 6339-6346.

[17] S.H. Wang, Y.L. Zi, Y.S. Zhou, S.M. Li, F.R. Fan, L. Lin, Z.L. Wang, J. Mater. Chem. A, 4 (2016) 3728-3734.

[18] J. Chen, H.Y. Guo, X.M. He, G.L. Liu, Y. Xi, H.F. Shi, C.G. Hu, ACS Appl. Mater. Interfaces, 8 (2016)

736-744.

[19] X.N. Xia, J. Chen, H.Y. Guo, G.L. Liu, D.P. Wei, Y. Xi, X. Wang, C.G. Hu, Nano Res., 10 (2017) 320-330.

[20] X.M. He, H.Y. Guo, X.L. Yue, J. Gao, Y. Xia, C.G. Hu, Nanoscale, 7 (2015) 1896-1903.

[21] Z. Wang, L. Cheng, Y.B. Zheng, Y. Qin, Z.L. Wang, Nano Energy, 10 (2014) 37-43.

[22] P. Bai, G. Zhu, Y.S. Zhou, S.H. Wang, J.S. Ma, G. Zhang, Z.L. Wang, Nano Res., 7 (2014) 990-997.

[23] F.R. Fan, W. Tang, Z.L. Wang, Adv. Mater., 28 (2016) 4283-4305.

[24] H.Y. Shao, Z. Wen, P. Cheng, N. Sun, Q.Q. Shen, C.J. Zhou, M.F. Peng, Y.Q. Yang, X.K. Xie, X.H. Sun, Nano Energy, 39 (2017) 608-615.

[25] L. Jin, W.L. Deng, Y.C. Su, Z. Xu, H. Meng, B. Wang, H.P. Zhang, B.B. Zhang, L. Zhang, X.B. Xiao, M.H. Zhu, W.Q. Yang, Nano Energy, 38 (2017) 185-192.

[26] L. Jin, J. Chen, B.B. Zhang, W.L. Deng, L. Zhang, H.T. Zhang, X. Huang, M.H. Zhu, W.Q. Yang, Z.L. Wang, ACS Nano, 10 (2016) 7874-7881.

[27] X.S. Zhang, M.D. Han, R.X. Wang, F.Y. Zhu, Z.H. Li, W. Wang, H.X. Zhang, Nano Lett., 13 (2013) 1168-1172.

[28] Y.B. Zheng, L. Cheng, M.M. Yuan, Z. Wang, L. Zhang, Y. Qin, T. Jing, Nanoscale, 6 (2014) 7842-7846.

[29] Y. Yang, H.L. Zhang, J. Chen, Q.S. Jing, Y.S. Zhou, X.N. Wen, Z.L. Wang, ACS Nano, 7 (2013) 7342-7351.

[30] S.M. Niu, X.F. Wang, F. Yi, Y.S. Zhou, Z.L. Wang, Nature communications, 6 (2015) 8.

[31] M.H. Yeh, H.Y. Guo, L. Lin, Z. Wen, Z.L. Li, C.G. Hu, Z.L. Wang, Adv. Funct. Mater., 26 (2016) 1054-1062.

[32] Y. Jie, N. Wang, X. Cao, Y. Xu, T. Li, X.J. Zhang, Z.L. Wang, ACS Nano, 9 (2015) 8376-8383.

[33] J. Wang, Z. Wen, Y.L. Zi, P.F. Zhou, J. Lin, H.Y. Guo, Y.L. Xu, Z.L. Wang, Adv. Funct. Mater., 26 (2016) 1070-1076.

[34] X.S. Zhang, J. Brugger, B. Kim, Nano Energy, 20 (2016) 37-47.

[35] H. Wang, M.Y. Shi, K. Zhu, Z.M. Su, X.L. Cheng, Y. Song, X.X. Chen, Z.Q. Liao, M. Zhang, H.X. Zhang, Nanoscale, 8 (2016) 18489-18494.

[36] J.K. Chen, H.W. Guo, P. Ding, R.Z. Pan, W.B. Wang, W.P. Xuan, X.Z. Wang, H. Jin, S.R. Dong, J.K. Luo, Nano Energy, 30 (2016) 235-241.

[37] N. Soin, P.F. Zhao, K. Prashanthi, J.K. Chen, P. Ding, E.P. Zhou, T. Shab, S.C. Ray, C. Tsonos, T. Thundat, E. Siores, J.K. Luo, Nano Energy, 30 (2016) 470-480.

[38] J.H. Lee, H.B. Lee, J.D. Andrade, Prog. Polym. Sci., 20 (1995) 1043-1079.

[39] N.Y. Cui, L. Gu, Y.M. Lei, J.M. Liu, Y. Qin, X.H. Ma, Y. Hao, Z.L. Wang, ACS Nano, 10 (2016) 6131-6138.

[40] Y.G. Feng, Y.B. Zheng, G. Zhang, D.A. Wang, F. Zhou, W.M. Liu, Nano Energy, 38 (2017) 27.

[41] S.M. Niu, S.H. Wang, L. Lin, Y. Liu, Y.S. Zhou, Y.F. Hu, Z.L. Wang, Energy Environ. Sci., 6 (2013) 3576-3583.

[42] K.E. Byun, Y. Cho, M. Seol, S. Kim, S.W. Kim, H.J. Shin, S. Park, S. Hwang, ACS Appl. Mater. Interfaces, 8 (2016) 18519-18525.

[43] W. Melitz, J. Shen, A.C. Kummel, S. Lee, Surf. Sci. Rep., 66 (2011) 1-27.

[44] D.W.V. Krevelen, K.T. Nijenhuis, Properties of Polymers, Springer-Verlag1980.

[45] J.E. Huheey, J. Phys. Chem., 69 (1965) 3284-&.

[46] A.F. Diaz, R.M. Felix-Navarro, J. Electrost., 62 (2004) 277-290.

[47] J.M. Wu, C.K. Chang, Y.T. Chang, Nano Energy, 19 (2016) 39-47.

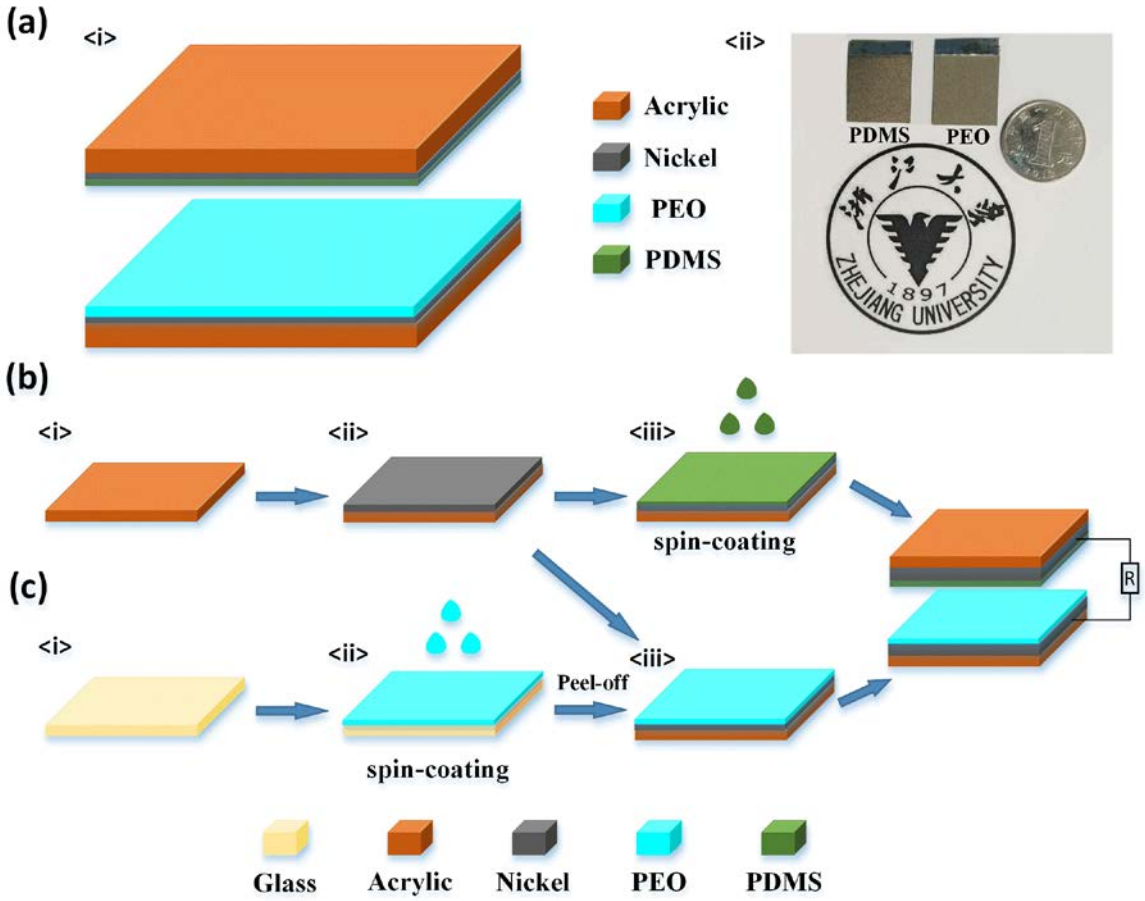

Fig. 1. Device structure, photo image and fabrication process of the TENG using PEO and PDMS films as the positive and negative tribo-materials, respectively. (a) Schematic diagram and a photo of the fabricated device, showing the structural design of the TENG, (b) and (c) fabrication flowchart for PDMS and PEO films, respectively.

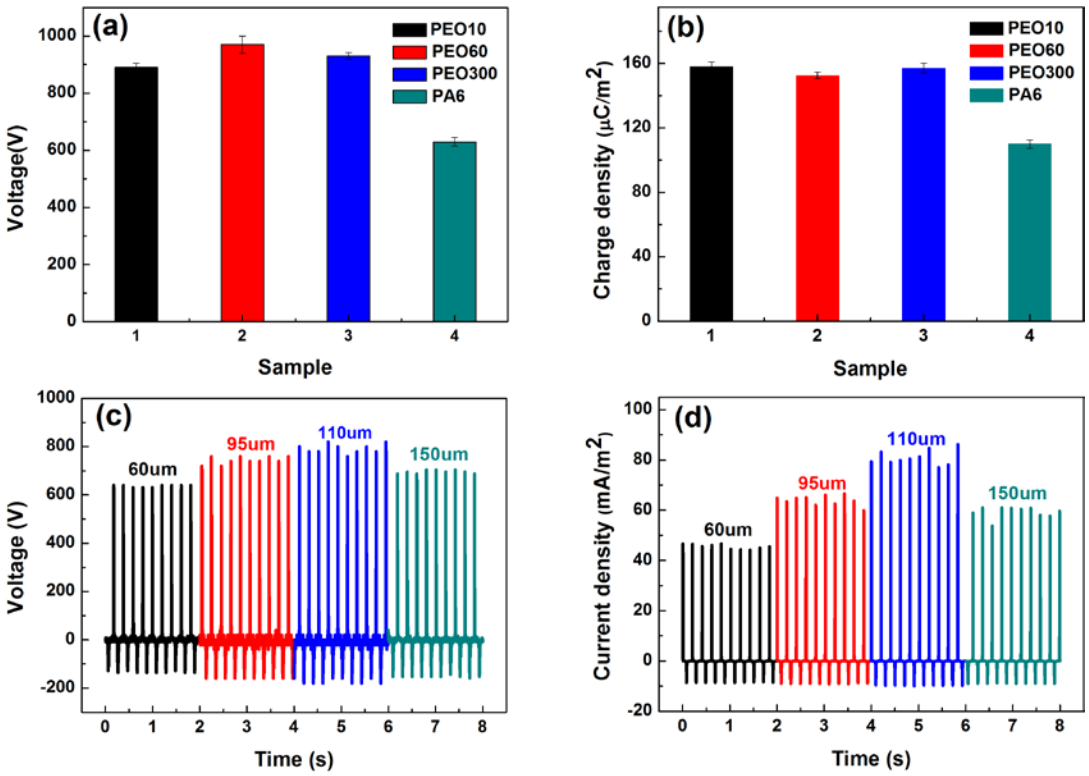

Fig. 2. Peak-to-peak open-circuit voltage (a) and charge density (b) obtained from the TENGs assembled using different molecular weights of PEO (Mw:10000-300000) in conjunction with PDMS. Comparison with the PA6/PDMS TENG is also shown in the same figures. The open-circuit voltage and current density of PEO60/PDMS TENGs with different PEO film thickness (60 μm, 95μm, 110 μm and 150 μm) are presented in (c) and (d) respectively, clearly showing the highest output values at 110 μm thickness.

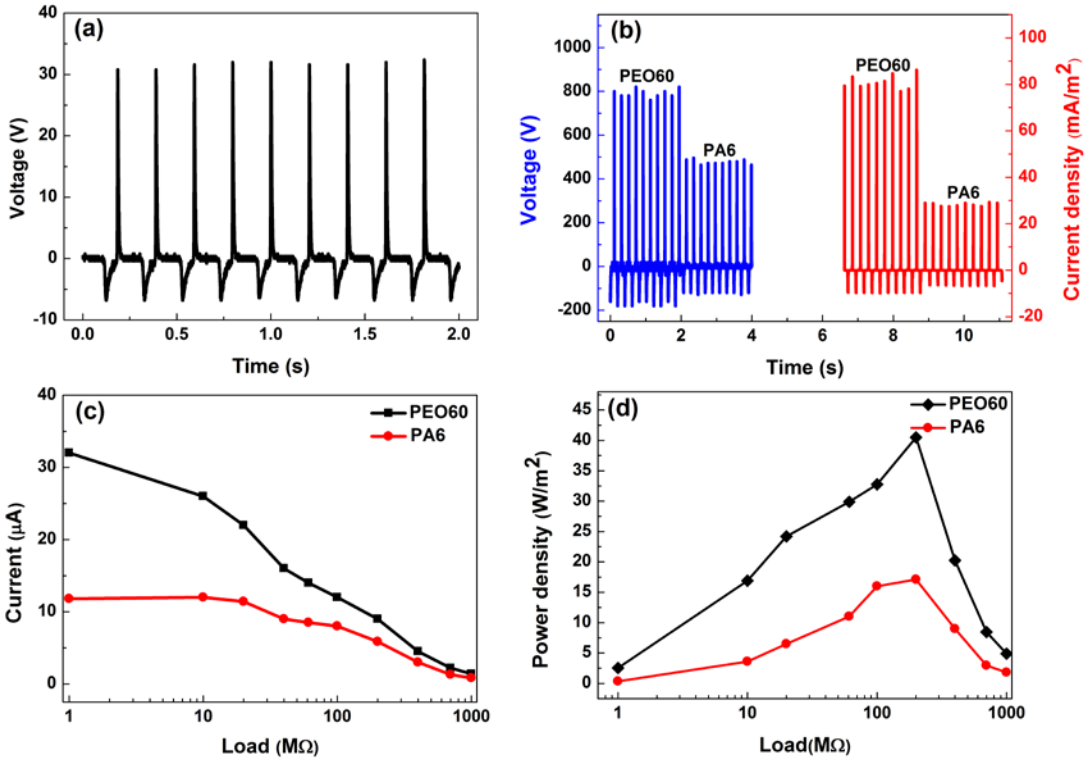

Fig. 3. (a) V_{OC} of the TENG composed of a PEO/PA6 material combination with the PEO side connecting to the (+), and PA6 to the (-) cable of the oscilloscope, (b) presents the specific V_{OC} and current density comparison between the PEO60/PDMS and PA6/PDMS TENGs, showing significantly higher performance for the PEO60/PDMS TENG than those of the PA6/PDMS TENG. (c) shows the short-circuit current and (d) the instantaneous peak power density of the PEO60/PDMS and PA6/PDMS TENGs as a function of electrical load. At the same load resistance of ~200 MΩ , the peak power density from the PEO/PDMS TENG is 40 Wm^{-2}, while that of the PA6/PDMS is only 18 Wm^{-2}.

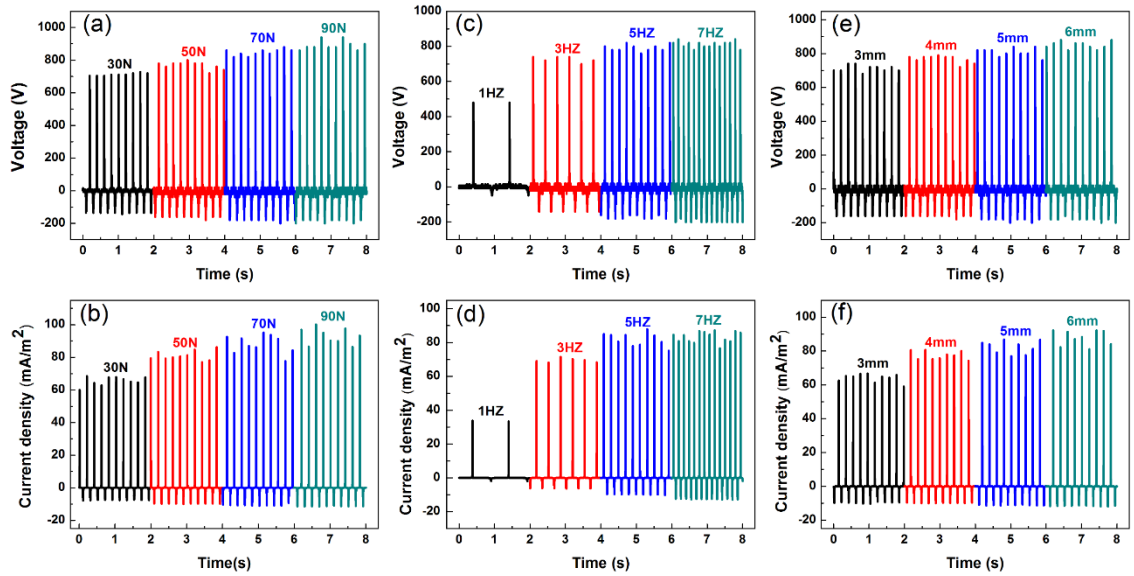

Fig. 4. Performance of the PEO60/PDMS TENG (with a 110 μm thickness PEO60 film), the open-circuit voltage (a) and current density (b) of the TENG under different contact forces, showing the similar increasing trend of outputs; influence of the contact frequency on the open-circuit voltage (c) and the current density (d), which increases when values of impact frequency is less than 5 Hz and saturates beyond that; the open-circuit voltage (e) and current density (f) with different spacer distances, again showing an increase with the increase of spacer distance.

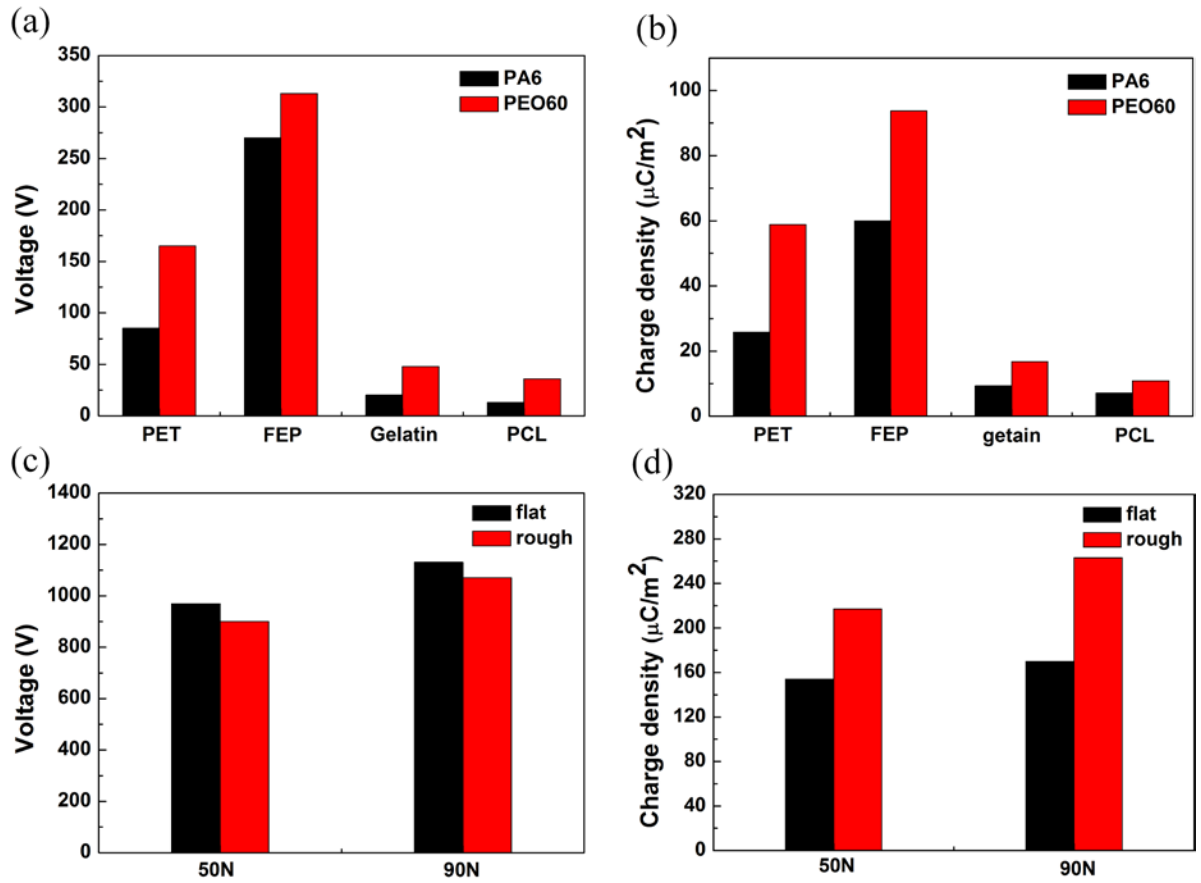

Fig 5. Output performance of TENGs assembled using various negative tribo-materials with PA6 and PEO60 films as the positive tribo-materials, respectively. The obtained peak-to-peak open-circuit voltage (a) and charge density (b) of the TENGs with PET, FEP, gelatin and PCl as the negative materials, respectively, clearly shows the higher positive electronic affinity for PEO; (c) the variation of peak-to-peak V_{OC} and (d) charge density of PEO/PDMS TENGs with different surface morphologies of PEO60 and PDMS films.

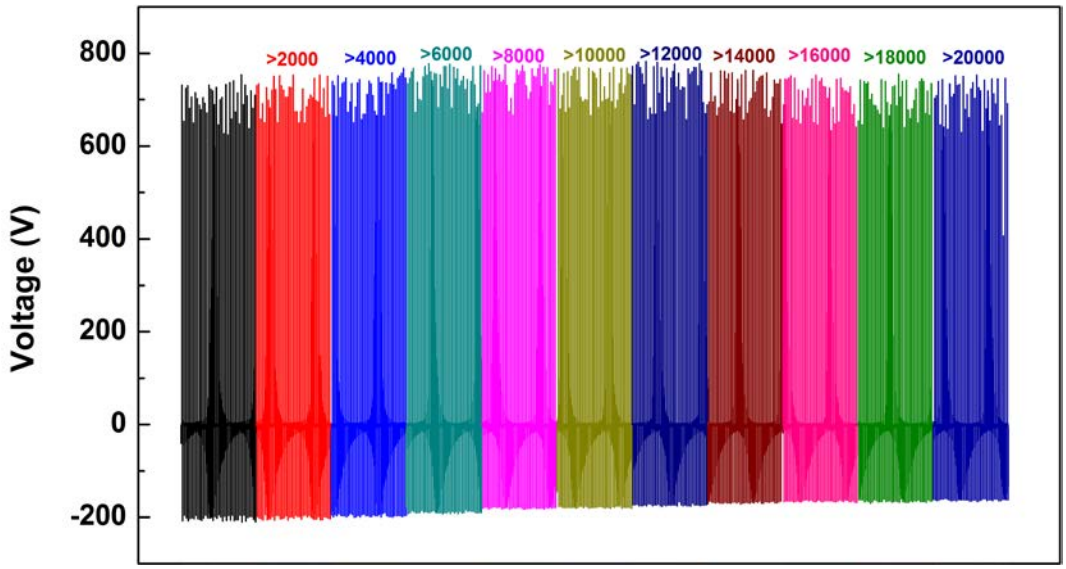

Fig. 6. Stability of a PEO60/PDMS TENG for more than 20000 energy generation cycles at a working frequency of 5 Hz, demonstrating its excellent stability.

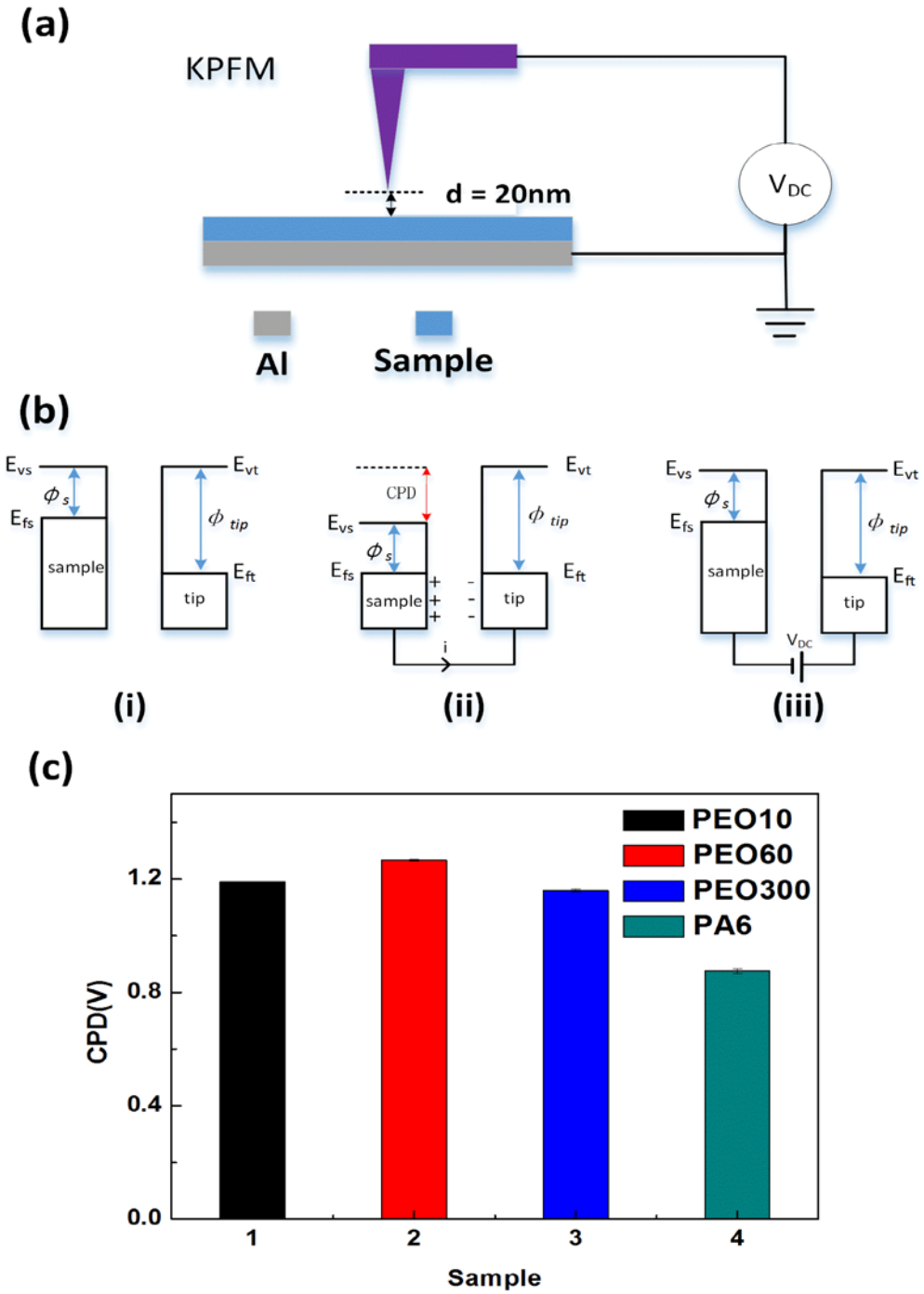

Fig. 7. Working principle and measurement result of KPFM characterization on the sample surface potential. (a) experimental setup of the KPFM; (b) working principle of the KPFM. An applied voltage on the tip is used to eliminate the potential difference; (c) the CPD histogram of KPFM measurement for PEO films with different molecular weights and PA6.

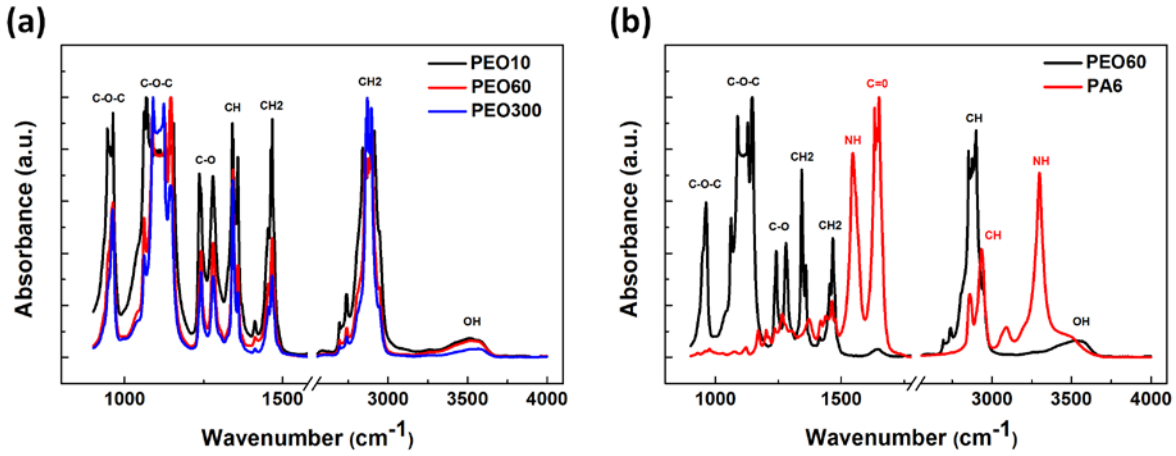

Fig. 8. FTIR measurement results for different molecular weights of PEO and PA6 polymers. Comparison of FTIR absorption spectra for (a) PEO with different molecular weights, (b) PEO60 and PA6.

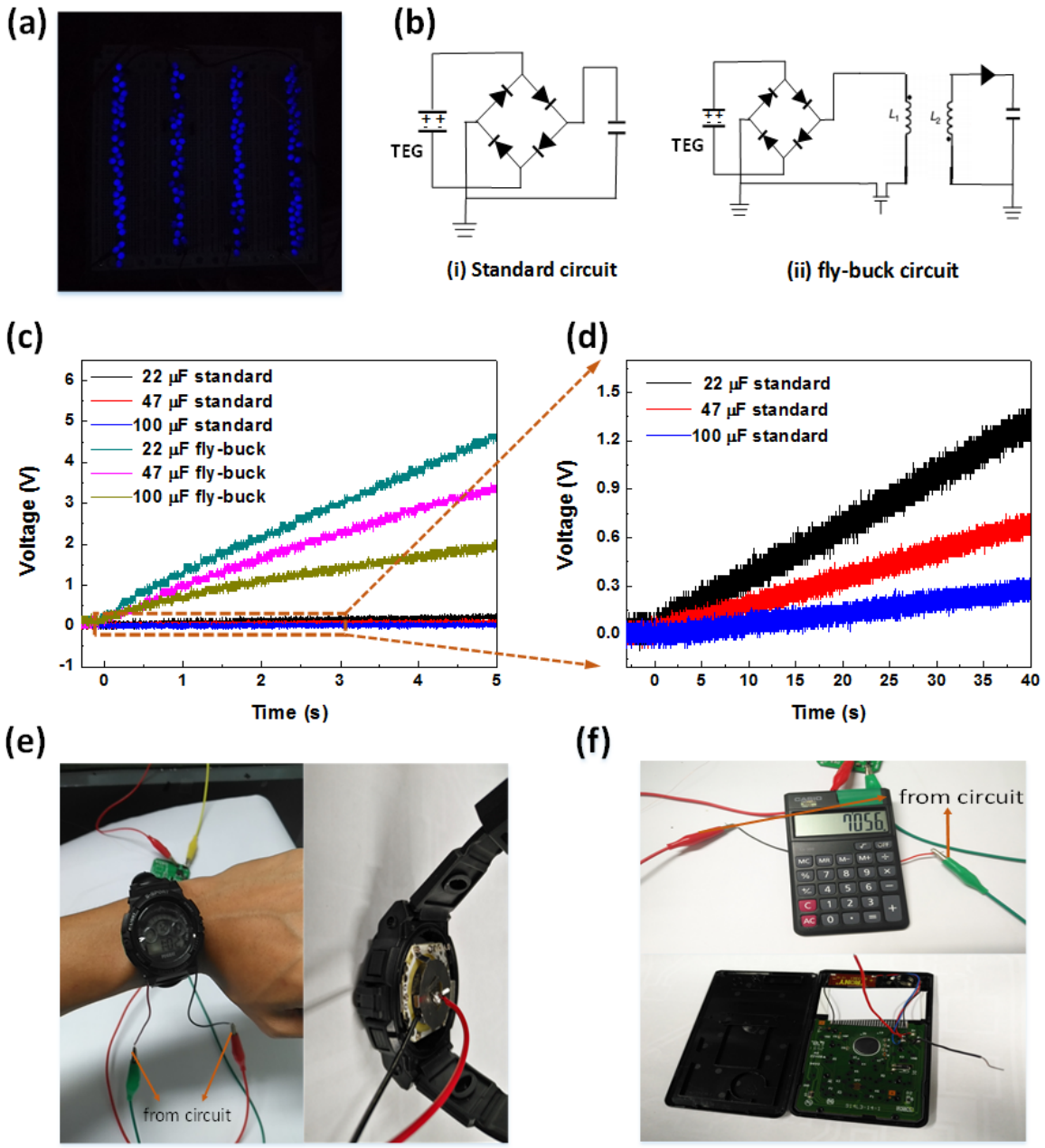

Fig. 9. Applications for a 2 ×2 cm^2 PEO60/PDMS TENG. (a) Hundreds of LEDs were directly powered by a TENG without any storage capacitor; (b) schematic diagram of the standard and fly-buck charging circuits for TENGs; (c) the comparative charge curves for 22 μF, 47 μF, 100 μF capacitors via the standard and fly-buck charging circuits using a PEO60/PDMS TENG are shown, wherein the fly-buck circuit shows a much faster charge speed; (d) an expanded view of the charge curves using the standard charging circuit shown in (b); and (e)-(f) a commercial calculator and a digital watch were powered by a 2 × 2 cm^2 PEO60/PDMS TENG under 2 Hz frequency whose internal coin cell had been removed.